

Topology Error Identification for Orthogonal Estimators Considering A Priori State Information

Antonio Simões Costa
Federal University of Santa Catarina
simoes@labspot.ufsc.br

Elizete Maria Lourenço
Federal University of Paraná
elizete@eletrica.ufpr.br

Fábio Vieira
Eletrosul Centrais Elétricas S.A.
fabiov@eletrosul.gov.br

Abstract - This paper addresses the problem of topology error identification for generalized orthogonal state estimators based on fast Givens rotations. Attention is focused on two issues: avoiding observability/criticality problems during topology error processing, and improving the performance of the error identification procedure. The former objective is attained by endowing the orthogonal estimator with a priori information processing capabilities. It is shown in the paper that prior knowledge on the states is easily accommodated in the three-multiplier Givens rotations framework, requiring no extra computational cost. To accomplish the second goal, we advocate the application of a geometric test to ensure that all devices with wrong status are duly selected as suspect. The effectiveness of the resulting identification method is assessed through its application to distinct situations involving topology errors simulated on the IEEE 24-bus test system.

Keywords - *Bad Data Analysis; Power System State Estimation; Power System Real-time Operation.*

1 Introduction

THE knowledge of the network topology is fundamental for real-time operation. All system based applications, such as state estimation, contingency analysis and on-line power flow, make use of the network topology defined by switch and circuit breaker status. Errors on those data produce incorrect topologies which, if undetected, will hamper the performance of subsequent EMS applications. Efficient tools to detect and identify topology errors are therefore instrumental to the power system real-time model building process.

Being widely recognized as an efficient tool to process gross errors on analog measurements, Power System State Estimation (PSSE) is a natural candidate to perform topology error identification. During the last decade, the emergence of the generalized state estimation approach [1] brought about a new generation of topology error algorithms. Those algorithms model selected regions of the network at the bus section level [2] and explicitly represent the status of switches and circuit-breakers (often referred to as *switching branches*). In [3], generalized state estimation is treated as a constrained minimization problem where measurement equations, null bus injections and switching branch status appear as equality constraints. The normalized Lagrange multipliers associated to switching branch status are then used to devise an enumerative method for detecting and identifying topology errors. An enhanced method is proposed in [4], where statistical tests assisted by a geometric approach eliminate the need of repeated state estimator runs, previously re-

quired in [3]. In [5], the numerical robustness of orthogonal methods is exploited to solve generalized state estimation, including topology error identification. Normalized residuals, instead of Lagrange multipliers, are used to select switching branches with suspect status. The conditional probability of each possible configuration involving the suspect set of devices is determined by the same hypothesis testing procedure used in [4]. As in [4], the correct topology is pointed out by the largest conditional probability of each candidate configuration, given the current set of measurement values.

A detrimental factor which often affects the performance of analytical approaches to topology error identification is the relatively lower level of measurement redundancy at the substation level, leading to the occurrence of critical constraints and critical sets of constraints [3]. Besides, when going through the various status configuration corresponding to distinct alternative hypothesis, observability problems may arise due to the creation of multiple observable islands, requiring the definition of multiple reference angles during topology error processing.

This paper proposes an improved version of the orthogonal method presented in [5], where topology error identification is carried out by Bayesian-based hypothesis testing. The main contributions of the paper are: *a)* the inclusion of *a priori* information in the orthogonal generalized formulation in order to avoid the need of defining multiple reference angles during the topology error process, and *b)* the use of a geometric test to ensure the selection of all wrongly modeled devices as suspect. The result is a more efficient and reliable topology error identification algorithm which eliminates islanding problems and reduces the effects of data criticality through the inclusion of *a priori* information, with no extra computational cost. Furthermore, the use of the geometric test has proved to be essential in cases where low redundancy tends to degrade normalized residual sensitivities.

The performance of the proposed method is assessed through its application to the IEEE 24-bus test system, considering different types of topology errors and distinct substation configurations.

2 Generalized State Estimation

2.1 Augmented State Vector - Operational and Structural Constraints

Assuming a linear (*DC*) model for a N bus power network on which m measurements are taken, the relationships between measurements and state variables can be

expressed as:

$$z_m = H_m x + \eta \quad (1)$$

where z_m is the $m \times 1$ measurement vector, H_m is an $m \times n$ measurement observation matrix, η is the $m \times 1$ measurement error vector and x is the $n \times 1$ state vector. We consider that x and H_m are augmented with respect to the conventional measurement model in order to include power flows on switching branches as new state variables [4]. Such an extension characterizes the so-called *Generalized State Estimation (GSE)*. Accordingly, the augmented state vector is defined as

$$x = [\delta^T, t^T]^T \quad (2)$$

where δ is an $(N - 1)$ -vector of bus voltage angles excluding the angle of the reference bus, t is the N_{sb} -vector of active flows through the modeled switching branches, and N_{sb} is the number of such branches. Thus, $n = N + N_{sb} - 1$ and matrix H_m contains additional columns with respect to the conventional observation matrix to account for the new state variables.

In order to represent the network at the substation level, two additional equations are required, as follows:

$$H_o x = 0 \quad (3)$$

$$H_s x = 0 \quad (4)$$

Eq. (3) models the status of switching branches, comprising zero voltage drops across closed switching branches ($\delta_i - \delta_j = 0$) and zero flows through open switching branches ($t_{ij} = 0$). Eq. (4) comprises deterministic information such as zero bus power injections at bus sections and bus voltage reference angles ($\delta_j = 0$).

Since we assume in this paper that both the measurements *and* the network topology are subject to uncertainty, the conventional state estimation weighted least-squares formulation is modified in order to include the status information given by Eq. (3) as pseudo-measurements. On the other hand, the deterministic information about zero bus injections and voltage reference angles are modeled as equality constraints. The state estimation problem is thus restated as:

$$\begin{aligned} \min \quad & \frac{1}{2}(z - H\hat{x})^T R^{-1} (z - H\hat{x}) \\ \text{s.t.} \quad & H_s \hat{x} = 0 \end{aligned} \quad (5)$$

where \hat{x} is the vector of state estimates, $z = [z_m^T \ 0]^T$ and

$$H = \begin{bmatrix} H_m \\ H_o \end{bmatrix} \quad R = \begin{bmatrix} R_m & 0 \\ 0 & R_o \end{bmatrix}$$

R_m is a diagonal matrix whose entries are the measurement variances, i.e., $R_m = \text{diag}\{\sigma_1^2, \dots, \sigma_m^2\}$. The $N_{sb} \times N_{sb}$ matrix R_o is the covariance matrix for the operational pseudo-measurements which is also assumed diagonal. The values of the corresponding variances reflect the level of uncertainty assigned to the status of network circuit-breakers and switches.

2.2 Embedding A Priori State Information

It is sometimes important to include in estimation process any *a priori* knowledge possibly available on the state variables. This can be implemented by adding to the objective function (5) a term of the form

$$\frac{1}{2}(\hat{x} - \bar{x})^T P^{-1} (\hat{x} - \bar{x}) \quad (6)$$

where \bar{x} is the vector of *a priori* information on the state variables and P is the corresponding covariance matrix. Typically, the values in \bar{x} are assumed uncorrelated, so that $P = \text{diag}\{\bar{\sigma}_1^2, \dots, \bar{\sigma}_n^2\}$, where $\bar{\sigma}_i^2$ models the uncertainty on the value of \bar{x}_i . Therefore, ascribing infinite values to $\bar{\sigma}_i^2$, $i = 1, \dots, n$, means that nothing is known in advance about the state variables. As a consequence, expression (6) is null, and the problem reduces itself to the conventional state estimation in which *a priori* information is not taken into account.

In most cases, however, some reliable knowledge is available about the states. For bus voltage angles, for instance, one can assume that they are in the vicinity of zero radian. In addition, under steady state conditions one can always define lower and upper bounds for θ_i , $i = 1, \dots, N$. For instance, it can be assumed that θ_i is uniformly distributed in the interval $[-\pi/2, \pi/2]$ rad. The latter argument allows the definition of matrix P , while the proximity of zero radian can be used to define the mean value \bar{x} . A similar reasoning can be used to define the mean values and variances for the remaining state variables.

A priori information on the states take part on the estimation procedure and ultimately affect the state estimates in precisely the same way as a set of additional direct pseudo-measurements of the state variables [6]. Such a property comes in handy when dealing with some practical situations, such as to circumvent the need of defining multiple angle references when islanding occurs, which is often the case during topology error processing. This topic will be re-examined in Section 3.

2.3 Normalized Residual for Topology Error Analysis

The solution of problem (5) provides estimation residuals for both analog measurements and switching branch statuses. Just as the former can be employed to detect bad data among measurements, the latter can be effectively used for topology error identification, as detailed in Section 4.

3 GSE via Givens Rotations

3.1 A Macro View

In this paper, the constrained weighted least-squares problem (5) is solved by the three-multiplier (*3-M*) version of Givens rotations [9]. To outline the procedure, consider that successive orthogonal transformations are applied to matrix H and vector z (both previously scaled by matrix $R^{-1/2}$) in order to obtain an upper triangular linear system of equations. If Q represents the matrix that stores the

individual rotations, we have [7],[8]:

$$Q (R^{-0.5} [H \mid z]) = \begin{bmatrix} U & c \\ 0 & d \end{bmatrix} \quad (7)$$

where U is an upper $n \times n$ triangular matrix and c is an n -vector. The fast versions of Givens rotations are based on the decomposition of matrix U as [9],[7]:

$$U = D^{\frac{1}{2}} \bar{U} \quad (8)$$

where D is a diagonal matrix and \bar{U} is a *unit* upper triangular matrix. Vector z is considered as extra column of H , so that the vector c is also scaled in the transformation. The resulting scaled vector is denoted by \bar{c} . The artifice of scaling U as above has a number of computational benefits, such as the elimination of square-root computations during the factorization given by Eq. 7. In practice, $D^{\frac{1}{2}}$ is not required, and only D needs to be computed. Further details on the elementary 3 - M Givens rotations are given in Subsection 3.2.

As long as the transformations (7) have been performed, the state estimates are obtained by simply solving the upper triangular system

$$\bar{U} \hat{x} = \bar{c} \quad (9)$$

by back-substitution. The weighted sum of squared residuals is determined from d , as a by-product of the estimation process.

The structural restrictions given by Eq. 4 are incorporated into the problem as equality constraints to the orthogonal estimation process and are dealt with by applying the iterative refinement weighting method described in [8].

The robustness of Givens rotations is particularly welcome in the present application, where weighting factor values for measurements and circuit-breaker status may considerably differ from each other.

3.2 The Elementary Rotations - Interpretation of Scaling Factors

In this subsection, we provide a “micro view” of the 3 - M Givens rotations, in order to show how this variant of the rotations provides a very simple means of incorporating *a priori* information into the estimation process.

To sequentially implement the scaling of matrix U as defined in Eq. (8), every new row of matrix H to be processed (augmented with the corresponding entry of vector z) is also assumed as scaled by a factor \sqrt{w} . Accordingly, prior to a particular rotation between a generic row \mathbf{h} and the i -th row \mathbf{u} of triangular matrix U aimed at zeroing out the i -th entry of \mathbf{h} , we have:

$$\begin{aligned} \mathbf{u} &= [0 \dots 0 \quad \sqrt{d} \quad \dots \quad \sqrt{d} \bar{u}_k \quad \dots \quad \sqrt{d} \bar{u}_{n+1}] \\ \mathbf{h} &= [0 \dots 0 \quad \sqrt{w} h_i \quad \dots \quad \sqrt{w} h_k \quad \dots \quad \sqrt{w} h_{n+1}] \end{aligned} \quad (10)$$

where \sqrt{d} is the current scaling factor of row \mathbf{u} of U . After applying the elementary rotation, \mathbf{u} and \mathbf{h} become:

$$\begin{aligned} \mathbf{u}' &= [0 \dots 0 \quad \sqrt{d'} \quad \dots \quad \sqrt{d'} \bar{u}'_k \quad \dots \quad \sqrt{d'} \bar{u}'_{n+1}] \\ \mathbf{h}' &= [0 \dots 0 \quad 0 \quad \dots \quad \sqrt{w'} h_k \quad \dots \quad \sqrt{w'} h'_{n+1}] \end{aligned}$$

The equations which define the relationships between the transformed and the original entries of \mathbf{u} and \mathbf{h} are given by [9]:

$$\begin{aligned} d' &= d + w h_i^2 \\ w' &= d w / d' \\ \bar{c} &= d / d' \\ \bar{s} &= w h_i / d' \end{aligned} \quad (11)$$

$$\left. \begin{aligned} h'_k &= h_k - h_i \bar{u}_k \\ \bar{u}'_k &= \bar{c} \bar{u}_k + \bar{s} h_k \end{aligned} \right\}, \quad k = i + 1 \dots n + 1 \quad (12)$$

where \bar{c} and \bar{s} are the parameters which define each elementary rotation. The 3 - M variant of Givens rotations owns its name from the name of multiplications required in the transformations in Eqs. (12). After the initialization of the weighting factors d and w , the rows of H are processed sequentially, each of them undergoing the number of elementary rotations necessary to annihilate all its nonzero entries. The rows of U , as well as matrix D , are updated during this process, through the above equations.

A very attractive feature of the 3 - M rotations is that the scaling mechanism required for their implementation allows the solution of *weighted* least squares problems for free, at no extra computational cost [9]. In PSSE problems, the value initially assigned to the row scaling factor w is the weight attributed to the corresponding measurement. That is, if row \mathbf{h} corresponds to, say, measurement z_j , then $w = 1/\sigma_j^2$ [7].

Having established the role of the measurement scaling factor w , an interpretation of the scaling factors d of the U rows is now in order. Analogy with w suggests that the initial value of d can also be seen as a weight, but in this case assigned to the states (notice that there are as many d 's as state variables) *before any measurement is processed*. In other words, d_i is the weighting factor for the *a priori* information possibly available on state variable x_i . In addition, the value for d_i must be in agreement with expression (6), which establishes how *a priori* information is taken into account in the estimation process. This leads to the conclusion that

$$d_i = 1/\bar{\sigma}_i^2 \quad (13)$$

where $\bar{\sigma}_i^2$ is the variance of the *a priori* information on state variable i .

The practice in previous applications of the 3 - M rotations to PSSE (which neglect *a priori* state information) has been to initialize $d_i = 0$ and $\bar{u}_{ii} = 1.0$ for every U row, which amounts to assuming that U is initially a null triangular matrix [7]. This is consistent with the discussion in Subsection 2.2, since such an initialization actually means that nothing is known in advance about the states, that is, their *a priori* variances are considered infinite.

To conclude, prior information on the states can be easily considered in the 3 - M Givens rotations framework by simply initializing the extra element \bar{u}_{n+1} in Eq. (10) as \bar{x}_i , and d_i as given by Eq. (13). Since the same variables already exist in the conventional formulation, with the only difference that they are initialized as zero, there is no extra computational cost for taking into account the *a priori* state information.

4 Topology Error Identification

4.1 Two-stage Strategy for Topology Error Identification

In this paper, we adopt the two-stage strategy for bad data processing proposed in [1]. In the first stage, the network is modeled at the bus-branch level and conventional state estimation is performed for the whole network. In case an error is detected, the region of the network where it occurs is identified as a “bad data pocket”. The second stage is then invoked in order to identify the error. It makes use of a detailed representation of the bad data pocket, whose substations are then modeled at the bus section level, as described in Section 2.

4.2 Role of the Generalized Normalized Residuals

As already mentioned, the GSE formulation of Section 2 provides a *generalized* vector of residuals, which comprises not only the residuals associated to analog measurements, but also those connected with status pseudo-measurements. Just as the former can be used to point out bad analog data, the latter can indicate inconsistencies in the network topology. Whatever the case, residuals must be normalized before bad data analysis is performed.

Upon solution of the state estimation problem (5) through the $3\text{-}M$ Givens rotations, the estimation residuals for both measurements (r_m) and status pseudo-measurements (r_o) are computed as:

$$r_m = z - H_m \hat{x} \quad (14)$$

$$r_o = -H_o \hat{x} \quad (15)$$

In order to normalized the residuals, the diagonal entries of the residual covariance matrix, denoted by C , are required. C can be computed in terms of matrices D and \bar{U} , as discussed in [7] and [5]. Its diagonal entries include both measurement and status pseudo-measurement variances, so that the residuals in Eqs. (14) and (15) can be normalized as:

$$r_m^N(i) = \frac{r_m(i)}{\sqrt{C^m(i,i)}} \quad \text{and} \quad r_o^N(i) = \frac{r_o(i)}{\sqrt{C^o(i,i)}} \quad (16)$$

where C^m and C^o are the diagonal blocks of C corresponding to analog measurements and status pseudo-measurements, respectively.

The occurrence of topology errors can now be detected by monitoring the residual $r_o^N(i)$ of largest absolute value. If it is found to be larger than a pre-specified threshold λ_t , it is concluded that a topology error has occurred. A typical threshold value is $\lambda_t = 3.0$.

4.3 Challenges to GSE-based Topology Error Identification

Topology error identification performed at the substation level is subject to some peculiar conditions which must be addressed when a methodology to tackle the problem is being devised. The most important are: *a*) Islanding problems during the execution of the topology error identification algorithm, and *b*) Occurrence of critical data and critical sets of data involving status pseudo-measurements.

The islanding issue naturally arises when one is dealing with distinct status configurations, since certain combinations of breaker status may lead to the formation of two or more electrical islands. A possible approach to deal with the problem is to dynamically identify the islands in order to define multiple reference angles, but this may be cumbersome to implement.

A much better solution is provided by the insertion of bus voltage angle *a priori* information in the estimation problem, as discussed in Subsection 3.2. With a proper definition of the corresponding weights d_i , such *a priori* data may function as *latent* reference angles for possibly occurring electrical islands. Accordingly, whenever the network behaves as a single integrated island the angle *a priori* information will have little effect on the estimates. Should however islanding conditions prevail, the *a priori* data ensures that state estimation can be performed without the need of defining multiple reference angles.

As for status pseudo-measurement criticality, it is to a large extent due to the topology of the reduced network under study, so that simply improving the metering scheme will have little or no effect to clear the problem [3]. Under such stringent conditions, hypothesis testing based on Bayes’ theorem has consistently shown good performance [4],[5].

4.4 Hypothesis Testing for Topology Error Identification

The Hypothesis Testing Identification (HTI) approach starts by partitioning the set of modeled circuit-breaker status into *suspect* (S) and *true* (T) subsets. This is a crucial step to ensure the proper HTI performance, since the inadvertent inclusion of erroneous data into set T instead of S violates a basic assumption and thus degrades the statistical properties of both sets [10]. Subset S is initially formed on the basis of the magnitudes of the normalized residuals r_o^N : status of breaker j is included in subset S if $r_o^N(j) > \lambda$, with λ defined as in Subsection 4.2. It should be mentioned, however, that such a procedure may not be sufficiently robust to ensure that S will contain all breaker with wrong status. This issue will be dealt with in Subsection 4.5.

Assuming that a reliable set of suspect circuit breaker status S has been determined, let n_s be the number of elements in S . We define the *null hypothesis* \mathcal{H}_0 as the combination of statuses originally used in setting up problem (5). Each of the remaining $2^{n_s} - 1$ status combinations constitute an *alternative hypothesis*.

The purpose of hypothesis testing is to establish if the observations processed by the state estimator support \mathcal{H}_0 or any of the alternative hypotheses \mathcal{H}_i . We make use of Bayes’ theorem [4] to decide which hypothesis is best supported by the observations. Let $P(\mathcal{H}_i)$ be the *a priori* probability and $P(\mathcal{H}_i | z)$ be the *a posteriori* probability of hypothesis \mathcal{H}_i . According to Bayes’ theorem, we have:

$$P(\mathcal{H}_i | z) = \frac{f(z | \mathcal{H}_i) P(\mathcal{H}_i)}{\sum_{j=1}^{n_s} f(z | \mathcal{H}_j) P(\mathcal{H}_j)} \quad (17)$$

where $f(z|\mathcal{H}_i)$ is the probability density function of z given that hypothesis \mathcal{H}_i holds. For each hypothesis, $f(z|\mathcal{H}_i)$ can be computed by using the orthogonal solution of problem (1) and proper forms of matrices H and R associated with hypothesis \mathcal{H}_i . As for the *a priori* probabilities $P(\mathcal{H}_i)$, their values should be provided as input data and can be determined from practical experience or from assumed probability values for breaker status [3].

It is important to remark that the calculation of a *posteriori* probabilities as given by Eq. (5) is based solely on the state estimation results for the null hypothesis. Therefore, no further state estimation runs for the alternative hypotheses are required, and $f(z|\mathcal{H}_i)$ is obtained from $f(z|\mathcal{H}_0)$ by modifying the corresponding covariance matrices [4].

4.5 Enhanced Selection of Suspect Devices

To make sure that all devices with wrong status are properly included in the suspect set S , we make use of a geometric test based on the orthogonal projection of the residuals onto the range space of the residual sensitivity matrix [12]. A similar test has been employed in [11], but that was applicable to Lagrange multipliers obtained from the sparse tableau state estimator.

The relationship between estimation residuals and the vector ϵ of errors on analog measurements and status pseudo-measurements is given by [10]

$$r = W \epsilon \quad (6)$$

where $r = [r_m^T, r_o^T]^T$ and W is the residual sensitivity matrix, which relates to the residual covariance matrix as $W = C R^{-1}$ [10]. Assume that the preliminary criterion based on the normalized residual magnitudes has been employed to label the data as *suspect* (S) or *free of bias* (T). If the columns of matrix W are partitioned accordingly, we have

$$W = [W_S \quad W_T] \quad (7)$$

Suppose that all analog measurements and status pseudo-measurements in T are perfect. In this case the error vector ϵ can be written as:

$$\epsilon = \begin{bmatrix} \epsilon_S \\ 0 \end{bmatrix} \quad (8)$$

When equations (7) and (8) are substituted in (6), we get:

$$r = W_S \epsilon_S \quad (9)$$

That is, if all erroneous information are included in the suspect set, vector r will lie in the range space of W_S . Consequently, the angle θ between r and its projection onto the range space of W_S will be zero, and consequently, $\cos \theta = 1$.

The above conclusion is based on the fact that data in set T are free of noise. However, in practice measurements are subject to random errors with zero mean and covariance matrix R_m so that the $\cos \theta$ value will not be exactly equal to 1.0, but will approach that value.

Let us now focus our attention on topology errors. Considering the partition of the residual vector into S and T subsets restricted to the *operational* pseudo-measurements, we have $r_o = [r_{o,S}^T, r_{o,T}^T]^T$. On the basis of the theoretic developments presented in [12] and [11], one can show that

$$\cos \theta = \sqrt{\frac{r_{o,S}^T (K_{ss})^{-1} r_{o,S}}{(r_o^T R r_o)}} \quad (10)$$

where $K_{ss} = (C_s^o)^T R^{-1} C_s^o$, and C_s^o is the partition of covariance matrix C^o corresponding to the suspect devices. Notice that the right-hand side of Eq. (10) is relatively simple to compute, so that the computational burden of implementing the cosine test is low.

To sum up, we propose the following procedure to enhance the suspect set pseudo-measurement selection. Eq. (10) is used to compute $\cos \theta$ considering the current partition of available data into suspect and true subsets. If the $\cos \theta$ value is sufficiently close to 1.0, i.e. $\cos \theta > 1 - \varepsilon$ where $\varepsilon \in [0.01, 0.1]$, we conclude that all erroneously modeled switching branches are in fact included in the suspect set, so that we can proceed with the hypothesis testing step. On the other hand, a value of $\cos \theta$ significantly different from 1.0 is an indication that not all switching branches with wrong *status* have been selected as suspect. The suspect set is then redefined by decreasing the threshold λ and the cosine-test is re-applied to the new suspect set. This procedure is repeated until the cosine-test is satisfied, i.e. until $\cos \theta \geq 1 - \varepsilon$.

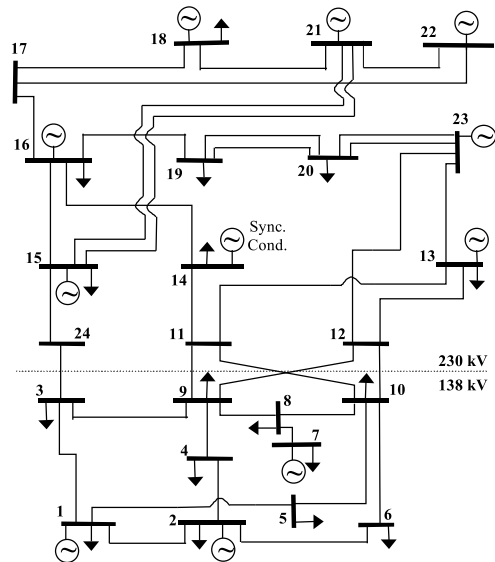


Figure 1: IEEE-24 bus test system

5 Simulation Results

The IEEE-24 bus test-system presented in Figure 1 is used to assess the performance of the proposed methodology for topology error identification. In the implementation, a linear version of the network is considered. As remarked in Subsection 4.1, the identification procedure is conducted in the second stage of the state estimation, so that suspect substations are represented at the bus section

level. In what follows, attention will be focussed on substations (STs) corresponding to buses 14, 15, 16 and 24 of the test system, whose description and substation data can be found in [13].

The tests conducted with the orthogonal estimator are based on the same topology errors simulated in [4], which employs a sparse tableau estimator. Simulation results are separated into two groups, A and B. Figures 2 and 3 show the detailed representation of the anomaly region for Cases A and B, respectively. The same conditions used in [4] are applied in the tests presented in this section, that is, the flow at both ends of all transmission lines and the injection at each bus are monitored, and measurements have been simulated as noisy, with covariances around 2% of the true values. *A priori* information are considered and modeled as described in Subsection 3.2. The actual *status* of the switching branches and those among them for which the power flow is monitored are represented in Figures 2 and 3.

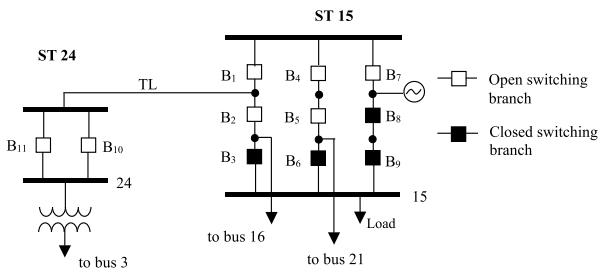


Figure 2: Anomaly region for Case A

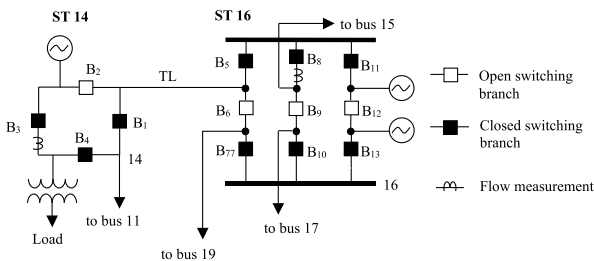


Figure 3: Anomaly region for Case B

Table 1 summarizes the simulated topology errors for Cases A and B. The second and third columns of the table show the error type and the circuit breakers (CBs) involved in each test. The correct and simulated *status* for those devices are presented in the two remaining columns of Table 1, where “0” and “1” represent open and closed *status*, respectively.

5.1 Case A

This section describes the results of a topology error of the inclusion type simulated on the network represented in Fig. 2. In what follows, f_{B_k} and $\Delta\delta_{B_k}$ stand for active power flow through and voltage angle difference across circuit breaker B_k , respectively.

Case	Error Type	CB	Status	
			Correct	Simulated
A	Inclusion	B_1	0	1
		B_7	0	1
		B_{10}	0	1
B	Multiple Exclusion	B_1	1	0
		B_5	1	0

Table 1: Simulated Topology Errors for Cases A and B

In Fig. 2, transmission line TL is out of service for the proposed operational condition, but the reported status of breakers B_1 , B_7 and B_{10} , which are wrongly assumed closed, bring about an inclusion error involving that branch. When the erroneous configuration is considered, those switching branches will be radially connected to the transmission line. The resulting criticality problem is circumvented by extending the corresponding anomaly zone [4].

Inclusion Error - Case A2			
Suspect Operational Constraints		Suspect Set	
$\lambda = 3.0$	$\cos \theta$		
$\Delta\delta_{B_1}=0$	$\Delta\delta_{B_8}=0$	0.9971	B_1 B_8
$\Delta\delta_{B_3}=0$	$\Delta\delta_{B_9}=0$		B_3 B_9
$\Delta\delta_{B_6}=0$	$\Delta\delta_{B_{10}}=0$		B_6 B_{10}
$\Delta\delta_{B_7}=0$			B_7

Table 2: Suspect Set Selection Results for Case A2

The suspect operational constraints selected with $\lambda_t = 3.0$ are shown in Table 2. The cosine test indicates that all erroneous constraints are included in the suspect set. the cosine value. Hypothesis testing is then performed on the *status* of the seven suspect devices. Notice that each alternative hypothesis results in a different network configuration, comprising different islanding and isolated nodes in the system. The use of *a priori* information as proposed in this paper avoids the need of identifying the connected network components and defining angle references for each of them.

Table 3 shows the largest conditional probability values obtained for this case. The value associated to the correct *status* of the suspect breakers is the largest among them, indicating that breakers B_1 , B_7 and B_{10} should be open, and at the same time confirming the assumed status for the remaining suspect devices.

Suspect Set Hypotheses: \mathcal{H}_i	$P(\mathcal{H}_i z)$
$\{B_1, B_3, B_6, B_7, B_8, B_9, B_{10}\}$	
$\{0\ 1\ 1\ 0\ 1\ 1\ 0\}$	0,99996
$\{0\ 1\ 1\ 0\ 1\ 1\ 1\}$	0,00001
$\{0\ 1\ 1\ 1\ 1\ 1\ 1\}$	0,00001

Table 3: Hypotheses Testing Results for Case A2

5.2 Case B

Case B consists of an exclusion error simulated in the anomaly zone shown in Figure 3. The transmission line referred to as TL in that figure is erroneously excluded from the system model. This error involves the *status* of circuit breakers B_1 and B_5 , which are reported as open to the state estimator. This case illustrates the importance of the collinearity test in topology error processing, as discussed

next.

The operational constraints selected as suspect using the first threshold ($\lambda = 3.0$) are shown in the first column of Table 4, while the corresponding cosine value obtained from the corresponding collinearity test appears in the second column. Since his value is significantly smaller than 1.0, one concludes that not all erroneous constraints have been properly selected. Threshold λ is then reduced until the collinearity test is satisfied, which occurs for $\lambda=0.5$. The remaining columns of table 4 show the suspect operational constraints, the corresponding cosine value, and the resulting suspect set, which contains the erroneous circuit breakers.

Exclusion Error - Case B2				
Suspect Operational Constraints				Suspect CB
$\lambda=3.0$	$\cos \theta$	$\lambda=0.5$	$\cos \theta$	
$f_{B_9} = 0$ $f_{B_{12}} = 0$	0.484	$f_{B_1} = 0$ $f_{B_5} = 0$ $f_{B_9} = 0$ $f_{B_{12}} = 0$	0.966	B_1 B_5 B_9 B_{12}

Table 4: Suspect Set Selection Results for Case B2

The conditional probability values are determined by applying the hypothesis testing on the suspect set, considering *a priori* information. They are found to be practically zero for all alternative hypotheses, except for hypothesis $\{1\ 1\ 0\ 0\}$ for which the conditional probability is equal to 1.0. This hypothesis represents the correct *status* combination for the suspect set of circuit breakers, thus identifying the exclusion error.

6 Conclusions

This paper introduces two improvements to topology error processing through Givens rotations-based generalized state estimators. The first one is the embedding of *a priori* state information into the orthogonal estimator framework. It is shown that the three-multiplier version of Givens rotations easily accommodates *a priori* information at virtually no extra cost. *A priori* data on bus voltage angles provide a convenient way of handling disjoint network components (islands) which usually occur in the course of topology error processing.

The second contribution enhances the performance of hypothesis testing for topology error identification by making sure that all devices with wrong status are included into the suspect set S submitted to the statistical tests. This is accomplished through a geometric procedure which is simple to implement and conclusive on the completeness of set S .

The combination of the various tools discussed in the paper has been applied to identify topology errors simulated on the IEEE-24 bus test system. A step-to-step account of the results is presented.

REFERENCES

[1] O. Alsaç, N. Vempati, B. Stott, and A. Monticelli. "Generalized State Estimation". *IEEE Trans. on*

Power Systems, 13(3):1069–1075, Aug. 1998.

- [2] A. Abur, H. Kim, and M. K. Celik. "Identifying the Unknown Circuit Breaker Statuses in Power Networks". *IEEE Trans. on Power Systems*, 10(4):2029–2037, Nov. 1995.
- [3] K. A. Clements and A. Simões Costa. "Topology Error Identification using Normalized Lagrange Multipliers". *IEEE Trans. on Power Systems*, 13(2):347–353, May 1998.
- [4] E. M. Lourenço, A. J. A. Simões Costa, and K. A. Clements. "Bayesian-Based Hypothesis Testing for Topological Error Identification in Generalized State Estimation". *IEEE Trans. on Power System*, 19(2):1206–1215, May. 2004.
- [5] A.J. Simões Costa and F. Vieira. "Topology Error Identification Through Orthogonal Estimation Methods and Hypothesis Testing". *IEEE Porto Power Tech, Porto, Portugal*, Sep. 2001.
- [6] P. Swerling. "Modern State Estimation Methods from the Viewpoint of the Method of Least Squares". *IEEE Trans. on Automatic Control*, AC-16(6):707–719, Dec. 1971.
- [7] A. J. A. Simões Costa, and V. H. Quintana. "An Orthogonal Row Processing Algorithm for Power System Sequential State Estimation". *IEEE Trans. on PAS*, 100(8):3791–3800, Aug. 1981.
- [8] A. J. A. Simões Costa, and J. P. Gouvêa. "A Constrained Orthogonal State Estimator for External System Modeling". *Int. J. on Electrical Power and Energy Systems*, 22(8):555–562, Nov. 2000.
- [9] W.M. Gentleman. "Least Squares Computations by Givens Transformations Without Square Roots". *Journal of the Inst. Math. Applics.*, AC-12:329–336, 1973.
- [10] L. Mili, and T. Van Cutsem, and M. Ribbens Pavella. "Hypothesis Testing Identification: A New Method for Bad Data Analysis in Power System State Estimation". *IEEE Trans. on PAS*, 103(11):3239–3252, Nov. 1984.
- [11] E. M. Lourenço, and K. A. Clements, and A. J. A. Simões Costa. "Geometrically-Based Hypothesis Testing for Topological Error Identification". *14th PSCC, Seville, Spain*, June 2002.
- [12] K.A. Clements, and P.W. Davis. "Multiple Bad Data Detectability and Identifiability: A Geometric Approach". *IEEE Trans. on Power Delivery*, 1(3):355–360, July 1986.
- [13] IEEE RTS Task Force of APM Subcommittee. "IEEE Reliability Test System". *IEEE Power Apparatus and Systems*, 98(6):2047–2054, Nov/Dec 1979.